Molecular Crystals and Liquid Crystals Science and Technology. Section A. Molecular Crystals and Liquid Crystals

Publication details, including instructions for authors and subscription information:
http://www.tandfonline.com/loi/gmcl19

Structural Behavior of n-Tricosane and n-Pentacosane Mixtures at 20°C

B. Jouti [a] , J. B. Bourdet [a] , M. Bouroukba [a] & M. Dirand [a]

[a] Laboratoire de Thermodynamique Chimique et Appliquée Ecole Nationale Supérieure des Industries Chimiques Institut National Polytechnique de Lorraine 1, rue Grandville-BP, 451-54001, Nancy Cédex, (France)

Version of record first published: 24 Sep 2006.

To cite this article: B. Jouti , J. B. Bourdet , M. Bouroukba & M. Dirand (1995): Structural Behavior of n-Tricosane and n-Pentacosane Mixtures at 20°C, Molecular Crystals and Liquid Crystals Science and Technology. Section A. Molecular Crystals and Liquid Crystals, 270:1, 159-173

To link to this article: http://dx.doi.org/10.1080/10587259508031025

Mol. Cryst. Liq. Cryst., 1995, Vol. 270, pp. 159–173
Reprints available directly from the publisher
Photocopying permitted by license only

Structural Behavior of *n*-Tricosane and *n*-Pentacosane Mixtures at 20°C

B. JOUTI, J.-B. BOURDET, M. BOUROUKBA and M. DIRAND

Laboratoire de Thermodynamique Chimique et Appliquée Ecole Nationale Supérieure des Industries Chimiques Institut National Polytechnique de Lorraine 1, rue Grandville-BP 451-54001 Nancy Cédex (France)

(Received March 13, 1995)

The study of the *n*-tricosane (*n*-$C_{23}H_{48}$): *n*-pentacosane (*n*-$C_{25}H_{52}$) mixtures was carried out using X-ray analyses. In spite of what is found in the literature, the X-ray diffraction results show the presence of six orthorhombic solid solutions when the molar concentration in *n*-pentacosane increases: three terminal solid solutions, denoted $\beta_0(C_{23})$, $\beta'_0(C_{23})$ and $\beta_0(C_{25})$, isostructural with *n*-tricosane and *n*-pentacosane structures and three orthorhombic intermediate phases, denoted β''_1, β' and β''_2. On the basis of powder X-ray patterns, the phases β''_1 and β''_2 are indistinguishable and they are isostructural with the solid solution β'' of the binary systems *n*-$C_{22}H_{46}$: *n*-$C_{24}H_{50}$ and *n*-$C_{24}H_{50}$: *n*-$C_{26}H_{54}$. The orthorhombic intermediate solid solution β' is also isostructural with the phases β'_1 and β'_2 of the binary systems *n*-$C_{22}H_{46}$: *n*-$C_{24}H_{50}$ and *n*-$C_{24}H_{50}$: *n*-$C_{26}H_{54}$. The six solid solutions ranges are determined by the X-ray patterns examination of twenty seven mixtures at 20°C.

Keywords: Powder X-ray diffraction, C_{23}, C_{25} *and* C_{23}:C_{25} *mixtures, intermediate solid solutions.*

INTRODUCTION

An estimate of the crystallisation point of fuels is possible only when the thermodynamic properties of the pure components and their respective mixtures are known. Moreover, the thermodynamic properties of normal paraffins are closely related to their structural properties. This has prompted a number of crystallographic studies with the aim of determining a relationships between properties and structures.

In our laboratory we are currently undertaking joint thermodynamic and structural studies on the liquid/solid and solid/solid equilibria occurring in the pure *n*-alkanes found in fuels[1–3] and in their mixtures.[4,5] The binary phase diagrams of two even-numbered *n*-alkanes [*n*-docosane (*n*-$C_{22}H_{46}$): *n*-tetracosane (*n*-$C_{24}H_{50}$)],[6,7] and [*n*-tetracosane (*n*-$C_{24}H_{50}$): *n*-hexacosane (*n*-$C_{26}H_{54}$)][8] and of an odd-numbered *n*-alkane with an even-numbered *n*-alkane [*n*-tricosane (*n*-$C_{23}H_{48}$): *n*-tetracosane (*n*-$C_{24}H_{50}$)][9] have been determined. In spite of what is generally found in the literature,[10–18] two consecutive even-numbered *n*-alkanes do not form a continuous homogeneous solid solution at "low temperature." The studies of Smith,[19] Luth,[20] Gerson and Nyburg,[21] and our laboratory[4–9] show the existence of two limited terminal solid solutions, which have the structure of the pure *n*-alkanes, and the presence of many orthorhombic intermediate phases.

This work deals with the structural behavior of the binary odd-numbered alkanes mixtures [*n*-tricosane(n-$C_{23}H_{48}$): *n*-pentacosane (n-$C_{25}H_{50}$)] (hereafter denoted by C_{23} and C_{25}) as a function of the molar concentration up to a concentration of 100% n-C_{25}, which has been studied by Retief *et al.*.[22]

EXPERIMENTAL METHODS

The mixtures have been prepared by melting together appropriate proportions of *n*-tricosane and *n*-pentacosane. The two *n*-paraffins were purchased from the Aldrich Chemical company; their purity grade was analysed by gas chromatography and was found to be 99% for *n*-pentacosane and over 99% for *n*-tricosane, respectively.

X-ray diffraction experiments were carried out on powder samples using the Cu K_α radiation. The X-ray patterns were made with a GUINIER DE WOLFF NONIUS camera, which provides both a clear separation of the wide angle BRAGG reflections and observation of the structural behavior with concentration. The exposure time was 24 h, using an X-beam, obtained with a 10 mA filament, at 50 kV voltage. The spacings on the X-ray patterns were measured with an accuracy of 0.25 mm for distances ranging from 10.5 to 125 millimeters. The calibration was obtained with spectroscopic pure gold as standard.

STRUCTURES OF TRICOSANE AND PENTACOSANE

Smith,[23] Teare,[24] Heyding,[25] Gerson,[26] Denicolo[27] have identified the structures of odd-numbered *n*-paraffins and allotted them the orthorhombic standard space group Pbcm n° 57.

At 20°C, the two *n*-paraffins (C_{23} and C_{25}) exhibit an orthorhombic (Pbcm) structure, denoted $\beta_o(C_{23})$ for the *n*-tricosane and $\beta_0(C_{25})$ for the *n*-pentacosane.

The lattice spacings determined both experimentally and by calculation, as well as the intensities of the BRAGG reflections obtained from the X-ray patterns (Fig. 1) performed at temperature 20°C and calculated are listed in Table I. The intensities were calculated with help of the Lazy Pulverix[28] program using the data (Pbcm) from Smith.[23]

Table II compares the experimental crystalline parameters of $\beta_0(C_{23})$ and $\beta_0(C_{25})$, with those published by Gerson.[26]

STRUCTURAL BEHAVIOR VERSUS C_{25} CONCENTRATION AT TEMPERATURE 20°C

Variations in the BRAGG diffraction patterns are noticeable on the X-ray photographs for molar concentrations of C_{25} of 2%, 3%, 30%, 50%, 80%, and 95% respectively (Fig. 1).

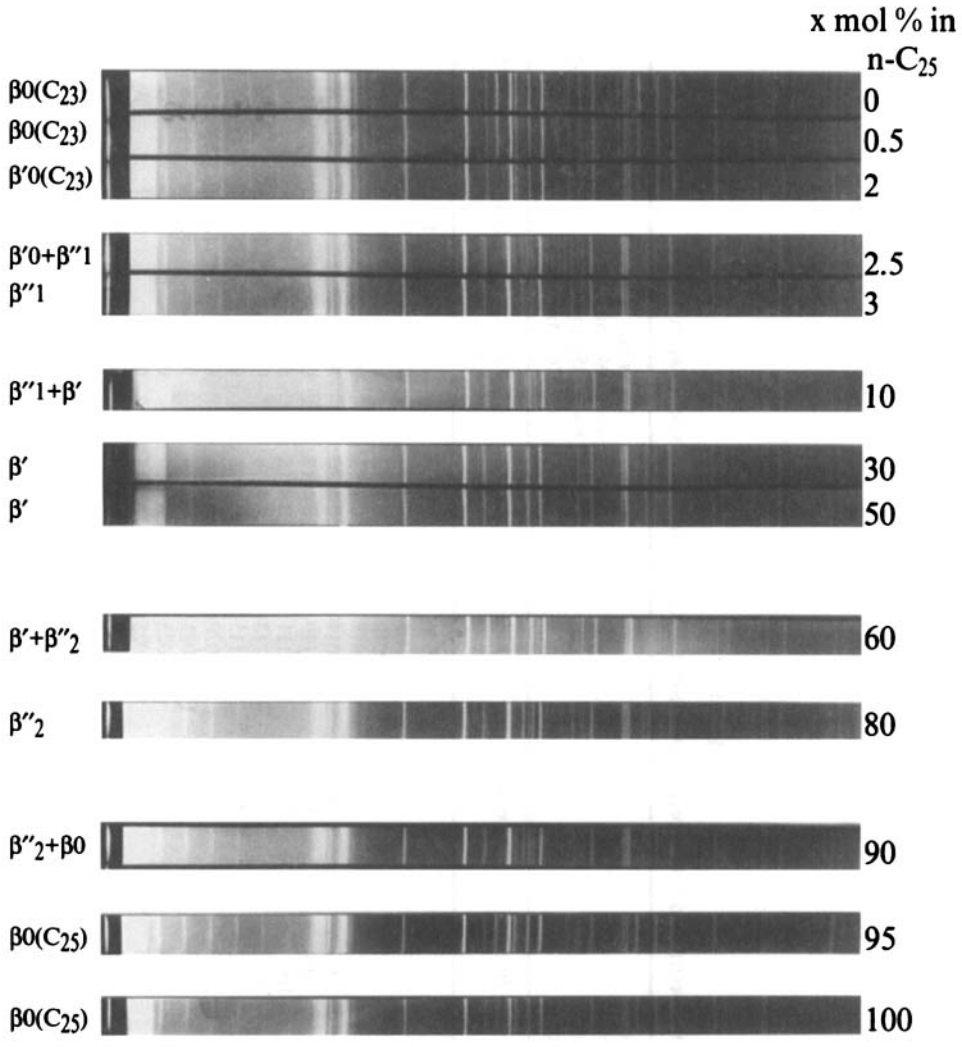

FIGURE 1 X-ray powder photographs taken with a Guinier de Wolff Nonius camera for several C_{23}–C_{25} mixtures when the molar concentration in *n*-pentacosane increases.

The lattice spacings and the intensities as experimentally recorded are listed in Table III and Table IV. These values demonstrate the existence of the four solid phases, denoted β'_0 (2%), β''_1 (3%), β' (30% and 50%), β''_2 (80%), and two terminal solid solutions $\beta_0(C_{23})$ and $\beta_0(C_{25})$ (95%).

The structures are orthorhombic with the parameters listed in Table III and Table IV. It is interesting to compare the results of the X-ray diffractions (Table III and Table IV) about the structures of these β'_0, β''_1, β', β''_2 phases, with the results obtained on powder samples of the terminal solid solutions $\beta_0(C_{23})$ and $\beta_0(C_{25})$.

TABLE I

Lattice spacing determined both experimentally from the X-ray patterns and by calculation

	Pentacosane $a = 0.496$ (nm) $b = 0.745$ (nm) $c = 6.7505$ (nm)					Tricosane $a = 0.494$ (nm) $b = 0.745$ (nm) $c = 6.226$ (nm)			
hkl	d (nm) exp	d (nm) calc	I(calc)	I(obser)	hkl	d (nm) exp	d (nm) calc	I(calc)	I
006	1.1210	1.1251	1.7	W	006	1.0393	1.038	1.7	
008	0.8482	0.8438	0.9	W	008	0.7806	0.778	0.9	
0010	0.6750	0.6751	0.5	W	0010	0.6242	0.623	0.5	
0012	0.5618	0.5625	0.3	W	0012	0.5173	0.519	0.3	
0014	0.4856	0.4822	0.2	W	0014	0.4430	0.447	0.2	
110	0.4150	0.4127	38.4	V-S	110	0.4115	0.412	38.3	
111	0.4150	0.4119	100	V-S	111	0.4115	0.411	100	
113	0.4059	0.4059	10.3	M	113	0.4036	0.404	10.2	
115	0.3947	0.3947	3.2	W	115	0.3918	0.391	3.1	
117	0.3795	0.3794	1.3	W	020	0.3724	0.372	12.3	
020	0.3732	0.3724	12.3	S	021	0.3724	0.372	32.6	
021	0.3732	0.3718	32.4	S	023	0.3656	0.366	3.5	
023	0.3675	0.3674	3.5	W	025	0.3548	0.356	1.2	
025	0.3593	0.3590	1.2	W	027	0.3430	0.343	0.5	
120	0.2973	0.2977	1.5	W	120	0.2971	0.297	1.5	
200	0.2479	0.2479	9.6	M	200	0.2471	0.247	9.5	
210	0.2348	0.2352	0.8	W	210	0.2345	0.235	0.8	
1026	0.2289	0.2300	3.3	M	1024	0.2286	0.230	3.3	
130	0.2213	0.2220	9.4	S	130	0.2211	0.222	9.4	

11 26	0.2188	0.2198	2.4	M	1124	0.2181	0.219	2.4
02 26	0.2117	0.2130	3.5	M	0224	0.2120	0.213	3.5
221	0.2059	0.2063	4.5	M	221	0.2056	0.206	4.5
12 25	0.1991	0.2000	1.0	W	1223	0.1995	0.199	1.0
12 26	0.1946	0.1957	0.6	W	1224	0.1944	0.194	0.6
12 27	0.1904	0.1915	0.7	W	1225	0.1898	0.189	0.7
041	0.1854	0.1861	0.9	W	041	0.1853	0.186	0.9
21 25	0.1765	0.1774	2.7	W	2123	0.1765	0.177	2.8
231	0.1748	0.1754	1.9	W	231	0.1745	0.175	1.9
21 26	0.1732	0.1743	1.9	W	2124	0.1733	0.174	1.9
13 25	0.1705	0.1715	3.6	M	1323	0.1700	0.171	3.6
13 27	0.1649	0.1660	2.8	M	1325	0.1646	0.165	2.8
22 26	0.1608	0.1615	1.3	M	2224	0.1605	0.161	1.3
04 26	0.1504	0.1513	3.3	M	0424	0.1504	0.151	3.3

W: Weak M: Medium S: Strong V-S: very strong

TABLE II

Lattice parameters of tricosane and pentacosane at 20°C

	$\beta_0(n\text{-}C_{23}H_{48})$		$\beta_0(n\text{-}C_{25}H_{52})$	
Parameters	This Work	GERSON (21)	This Work	GERSON (21)
a(nm)	0.494	0.4968	0.496	0.4962
b(nm)	0.745	0.7441	0.745	0.7442
c(nm)	6.226	6.2369	6.7505	6.724
α(°)	90	90	90	90
β(°)	90	90	90	90
γ(°)	90	90	90	90

A COMPARISON BETWEEN THE X-RAY PATTERNS OF β'_0 $\beta_0(C_{23})$ AND $\beta'_0(C_{23})$

Variation of the X-ray patterns from the terminal solid solution $\beta_0(C_{23})$ to β'_0 versus the C_{25} concentration

The behavior of the "low temperature" orthorhombic structure of tricosane, noted $\beta_0(C_{23})$, with the Pbcm space group[23,24] as observed on the mixture with the molar concentration 0.5% C_{25}, varies when the molar concentration of C_{25} is equal to 2% (Fig. 1, Table III):

i) the lines $d = 0.229$ nm (1 0 24), 0.1765 nm (2 1 23) disappear
ii) the lines $d = 0.237$ nm, 0.1675 nm appear
iii) the intensity of the BRAGG diffractions $d = 0.221$ nm(1 3 0) increases.

Similarity between β'_0 and $\beta'_0(C_{23})$

The above modifications are similar to those recorded by UNGAR[29,30] and HASNAOUI[5] in their studies of the pure C_{23} structural behavior as a function of temperature. In this particular case, they also correspond to the δ transition: $\beta_0(C_{23}) \rightarrow \beta'_0(C_{23})$, as observed by SNYDER[31]. These observations allow us to say that the $\beta'_0(C_{23})$ and the β'_0 are identical. The phase β'_0 in the mixture is actually the solid high temperature terminal solution of C_{25} in $\beta'_0(C_{23})$. An increase in the disorder of the crystallographic structure of C_{23} is produced by the presence of a few percent of C_{25} which can therefore be said to have the same effect as temperature; this behavior has also been observed in the binary mixtures [C_{23}:C_{24}] by SABOUR[9], when the concentration of C_{24} increases in C_{23}.

STRUCTURAL VARIATIONS FROM THE TERMINAL PHASE β'_0 TO THE INTERMEDIATE PHASE β''_1

The mixture with a molar concentration of 3% C_{25} exhibits the orthorhombic structure of the intermediate β''_1 phase. As compared with β'_0, this is reflected by the

following modifications of the X-ray patterns [(Fig. 1) and Table III]. The lines corresponding to the following *d* values disappear: 0.219 nm (1 1 24), 0.200 nm (1 2 23), 0.195 nm (1 2 24), 0.190 nm (1 2 25), 0.170 nm (1 3 23), 0.165 nm (1 3 25), while the lines corresponding to the following *d* values appear: 0.215 nm, 0.210 nm, 0.203 nm, 0.198 nm, 0.193 nm, 0.189 nm, 0.170 nm, 0.167 nm.

STRUCTURAL VARIATIONS FROM β_1'' TO β'

The mixture with a molar concentration of 30% C_{25} exhibits the orthorhombic structure of the intermediate phase β'. As compared with the β_1'' phase, this is reflected by the following values [(Figure 1) and Table III].

i) the lines corresponding to the following *d* values disappear: 0.167 nm, 0.1675 nm, 0.170 nm, 0.189 nm, 0.193 nm, 0.198 nm, 0.203 nm, 0.210 nm, 0.215 nm.
ii) while the lines corresponding to the following *d* values appear: 0.164 nm, 0.165 nm, 0.168 nm, 0.191 nm, 0.195 nm, 0.199 nm, 0.201 nm.

STRUCTURAL VARIATIONS FROM β_2'' TO β'

The mixture with a molar concentration of 80% C_{25} exhibits the orthorhombic structure of the intermediate phase β_2'' (Table IV, Fig. 1).

On the basis of powder X-ray diffraction photographs (Fig. 1, Table IV), both β_1'' and β_2'' intermediate solid solutions are indistinguishable except when considering the *c* parameter variation, thus they are isostructural.

The variations of the X-ray patterns between β_2'' and β' intermediate solid solutions are identical to those observed with β_1'' and β' (Fig. 1, Table III and IV).

STRUCTURAL VARIATIONS FROM THE TERMINAL SOLID SOLUTION $\beta_0(C_{25})$ TO THE INTERMEDIATE PHASE β_2''

The behavior of the low temperature orthorhombic structure (space group Pbcm[23,24]) of C_{25}, noted $\beta_0(C_{25})$, is characterised for a mixture with a molar concentration of 95% C_{25} as shown in Figure 1 and Table IV. When the molar concentration of C_{25} decreases from 95 to 80%, the following modifications of the X-ray patterns have been observed:

i) the lines corresponding to the following *d* values disappear: 0.229 nm (1 0 26), 0.219 nm (1 1 26), 0.199 nm (1 2 25), 0.195 nm (1 2 26), 0.190 nm (1 2 27), 0.1765 nm (2 1 25), 0.1705 nm (1 3 25), 0.165 nm (1 3 27).
ii) while the lines corresponding to the following *d* values appear: 0.214 nm, 0.210 nm, 0.203 nm, 0.197 nm, 0.192 nm, 0.189 nm, 0.1685 nm, 0.167 nm, 0.1665 nm.
iii) the intensity of the BRAGG diffractions corresponding to $d = 0.221$ nm (1 3 0) increases (Fig. 1, Table IV).

TABLE III

Lattice spacing both experimentally determined and calculated, (h k l) index of reflection intensities estimated for $\beta_0(C_{23})$, $\beta'_0(2\%)$, $\beta''_1(3\%)$,

	Phase β_0 *n*-tircosane $a = 0.494$ (nm) $b = 0.745$ (nm) $c = 6.226$ (nm)				Phase β'_0 (2% in C_{25}) $a = 0.494$ (nm) $b = 0.745$ (nm) $c = 6.229$ (nm)				Phase β''_1 (3% in C_{25}) $a = 0.494$ (nm) $b = 0.745$ (nm) $c = 6.288$ (nm)				Ph (30% $a = 0$ $b = 0$ $c = 6$	
hkl	d (nm) exp	d (nm) calc	I obs	I calc	d (nm) exp	d (nm) calc	I obs	I calc	d (nm) exp	d (nm) calc	I obs	I calc	d (nm) exp	d (r ca
006	1.0393	1.0377	W	1.7	1.0406	1.038	W	1.7	1.0486	1.048	W	1.7	1.0806	1.0
008	0.7806	0.7783	W	0.9	0.7813	0.7786	W	0.9	0.7875	0.7860	W	0.9	0.8109	0.8
0010	0.6242	0.6226	W	0.5	0.6242	0.6229	W	0.5	0.6297	0.6288	W	0.5	0.6493	0.6
0012	0.5173	0.5188	W	0.3	0.5176	0.5191	W	0.3	0.5234	0.5240	W	0.3	0.5400	0.5
0014	0.4430	0.4447	W	0.2	0.4430	0.4449	W	0.2	0.4480	0.4491	W	0.2	0.4630	0.4
110	0.4115	0.4117	V-S	-38	0.4115	0.4118	V-S	38.3	0.4115	0.4118	V-S	38.3	0.4129	0.4
111	0.4115	0.4109	V-S	100	0.4115	0.4108	V-S	100	0.4115	0.4109	V-S	100	0.4129	0.4
113	0.4036	0.4039	M	10.2	0.4041	0.4039	M	10.2	0.4050	0.4040	M	10.2	0.4055	0.4
115	0.3918	0.3909	W	3.1	0.3927	0.3909	W	3.1	0.3931	0.3913	W	3.1	0.3939	0.3
020	0.3724	0.3723	S	12.9	0.3724	0.3723	S	12.3	0.3724	0.372	S	12.3	0.3724	0.3
021	0.3724	0.3717	S	32.6	0.3724	0.3723	S	32.6	0.3724	0.372	S	32.6	0.3724	0.3
023	0.3656	0.3665	W	3.5	0.3659	0.3665	W	3.5	0.3659	0.3666	W	3.5	0.366	0.3
025	0.3548	0.3567	W	1.2	0.3552	0.3567	W	1.2	0.3552	0.3570	W	1.2	0.3552	0.3
027	0.3430	0.3435	W	0.5	0.3434	0.3435	W	0.5	0.3437	0.3439	W	0.5	0.3437	0.3
120	0.2971	0.2974	W	1.5	0.2971	0.2974	W	1.5	0.2976	0.2974	W	1.5	0.2976	0.2
200	0.2471	0.2471	M	9.5	0.2471	0.2471	M	9.5	0.2471	0.2471	M	9.5	0.2471	0.2
*	—	—			0.2372		W		0.2373		W		0.2372	
210	0.2345	0.2345	W	0.8	0.2345	0.2345	W	0.8	0.2345	0.2345	W	0.8	0.2351	0.2
10 24*	0.2286	0.2297	M	3.3	—	—	—	—	—	—	—	—	—	
130	0.2211	0.2218	S	9.4	0.2214	0.2218	S	9.4	0.2215	0.2218	S	9.4	0.2216	0.2
11 24**	0.2181	0.2195	M	2.4	0.2186	0.2196	M	2.4	—	—			—	
**$	—	—			—	—			0.2149		M		—	
02 24	0.2120	0.2128	M	3.5	0.2123	0.2129	M	3.5	0.2123	0.2129	M	3.5	0.2123	0.2
**$	—	—			—	—			0.2102		M		—	
221	0.2056	0.2058	M	4.5	0.2057	0.2057	M	4.5	0.2056	0.2057	M	4.5	0.2060	0.2
**$	—	—			—	—			0.2034				—	
12 23**	0.1995	0.2002	W	1.0	0.2000	0.2002	W	1.0	—	—			—	

$	—	—			—	—			—	—			0.2007	
$	—	—			—	—			—	—			0.1992	
**$	—	—			—	—			0.1981		W		—	
12 24**	0.1944	0.1955	W	0.6	0.1948	0.1955	W	0.6	—	—			—	
$	—	—			—	—			—	—			0.1946	
**$	—	—			—	—			0.1927		W		—	
12 25**	0.1898	0.1909	W	0.7	0.1903	0.1909	W	0.7	—	—			—	
$	—	—			—	—			—	—			0.1907	
**$	—	—			—	—			0.1889		W		—	
041	0.1853	0.1861	W	0.9	0.1854	0.1861	W	0.9	0.1859	0.186	W	0.9	0.1857	0.18
21 23*	0.1765	0.1772	W	2.8	—	—	—		—	—	—		—	
231	0.1745	0.1751	W	1.9	0.1749	0.175	W	1.9	0.1752	0.175	W	1.9	0.1753	0.17
21 24	0.1733	0.1739	W	1.9	0.1737	0.174	W	1.9	0.1737	0.174	W	1.9	0.1738	0.17
13 23**	0.1700	0.1716	M	3.6	0.1704	0.171	M	3.6	—	—			—	
**$	—	—			—	—			0.1696		W		—	
$	—	—			—	—			—	—			0.1678	
*$	—	—			0.1675				0.1675		W		—	
**$	—	—			—	—			0.1672		W		—	
$	—	—			—	—			—	—			0.1653	
13 25**$	0.1646	0.1656	M	2.8	0.1650	0.165	M	2.8	—	—			0.164	0.16
22 24	0.1605	0.1613	M	1.3	0.1608	0.161	M	1.3	0.1613	0.161	M	1.3	0.1614	0.16
04 24	0.1504	0.1513	M	3.5	0.1506	0.151	M	3.5	0.1507	0.151	M	3.5	0.1507	0.15

* denotes the lines which characterize the transition (β_0–β'_0)
** denotes the lines which characterize the transition (β'_0–β''_1)
$ denotes the lines which characterize the transition (β''_1–β')
V-S: Line of very strong intensity
S: Line of strong intensity
M: Line of medium intensity
W: Line of weak intensity

TABLE IV

Lattice spacing both experimentally determined and calculated, (hkl) index of reflection intensities estimated for $\beta_0(C_{25})$, $\beta_0(95\%)$, $\beta_2''(80\%)$,

	Phase β_0 *n*-pentacosane $a = 0.496$ (nm) $b = 0.745$ (nm) $c = 6.7505$ (nm)				Phase β_0 (95% in C_{25}) $a = 0.496$ (nm) $b = 0.745$ (nm) $c = 6.728$ (nm)				Phase β_2'' (80% in C_{25}) $a = 0.495$ (nm) $b = 0.745$ (nm) $c = 6.712$ (nm)				Phase β (50% in C $a = 0.495$ $b = 0.745$ $c = 6.656$	
hkl	d (nm) exp	d (nm) calc	I obs	I cal	d (nm) exp	d (nm) calc	I obs	I calc	d (nm) exp	d (nm) calc	I obs	I cal	d (nm) exp	d (nm) calc
006	1.1210	1.1251	W	1.7	1.119	1.251	W	1.7	1.1181	1.1186	W	1.7	1.1146	1.1093
008	0.8482	0.8438	W	0.9	0.846	0.8438	W	0.9	0.8417	0.8390	W	0.9	0.8319	0.8320
0010	0.6750	0.6751	W	0.5	0.672	0.6751	W	0.5	0.6651	0.6712	W	0.5	0.6626	0.6656
0012	0.5618	0.5625	W	0.3	0.5602	0.5625	W	0.3	0.5621	0.5593	W	0.3	0.5540	0.5546
0014	0.4856	0.4822	W	0.2	0.4810	0.4822	W	0.2	0.4800	0.4794	W	0.2	0.4750	0.4754
110	0.4135	0.4127	V-S	38.4	0.4135	0.4127	V-S	38.4	0.4131	0.4125	V-S	38.5	0.4133	0.4122
111	0.4135	0.4119	V-S	100	0.4135	0.4119	V-S	100	0.4131	0.4117	V-S	100	0.4133	0.4114
113	0.4059	0.4059	M	10.3	0.4052	0.4059	M	10.3	0.4046	0.4056	M	10.4	0.4060	0.4053
115	0.3947	0.3947	W	3.2	0.3942	0.3947	W	3.2	0.3939	0.3943	W	3.2	0.3932	0.3938
117	0.3795	0.3794	W	1.3	0.3788	0.3794	W	1.3	0.3780	0.3789	W	1.3	0.3777	0.3782
020	0.3723	0.3724	S	12.3	0.3723	0.3724	S	12.3	0.3723	0.3724	S	12.3	0.3723	0.3723
021	0.3723	0.3718	S	32.4	0.3723	0.3718	S	32.4	0.3723	0.3718	S	32.4	0.3723	0.3718
023	0.3675	0.3674	W	3.5	0.3669	0.3674	W	3.5	0.3665	0.3673	W	3.5	0.3668	0.3672
025	0.3593	0.3590	W	1.2	0.359	0.3590	W	1.2	0.3585	0.3588	W	1.2	0.3577	0.3586
120	0.2973	0.2977	W	1.5	0.2973	0.2977	W	1.5	0.2970	0.2977	W	1.5	0.2981	0.2976
200	0.2479	0.2479	M	9.6	0.2479	0.2479	M	9.6	0.2477	0.2477	M	9.6	0.2475	0.2475
**									0.2377		W		0.2476	
210	0.2348	0.2352	W	0.8	0.2346	0.2352	W	0.8	0.2348	0.2350	W	0.8	0.2355	0.2349
1026**	0.2289	0.2300	M	3.3	0.2283	0.2300	M	3.3	—					
130	0.2213	0.2220	S	9.4	0.2211	0.2220	S	9.4	0.2212	0.2219	S	9.4	0.2221	0.2219
1126**	0.2188	0.2198	M	2.4	0.2175	0.2198	M	2.4	—					
**$									0.2140		W			
0226	0.2117	0.2130	M	3.5	0.2118	0.2130	M	3.5	0.2115	0.2122	M	3.4	0.2118	0.2109
**$									0.2100		W			
221	0.2059	0.2063	M	4.5	0.2056	0.2063	M	4.5	0.2053	0.2061	M	4.5	0.2065	0.2060
**$									0.2034		W			
1225**	0.1991	0.2000	W	1.0	0.1985	0.2000	W	1.0	—					

$													0.2013	
$													0.1995	
**$									0.1969		W			
1226**	0.1946	0.1957	W	0.6	0.1942	0.1957	W	0.6	—					
$													0.1945	
**$									0.1922		W			
1227**	0.1904	0.1915	W	0.7	0.1900	0.1915	W	0.7	—					
$													0.1909	
**$									0.1891		W			
041	0.1854	0.1861	W	0.9	0.1852	0.1861	W	0.9	0.1850	0.1861	W	0.9	0.1862	0.1861
2125**	0.1765	0.1774	W	2.7	0.1762	0.1774	W	2.7	—					
231	0.1748	0.1754	W	1.9	0.1746	0.1754	W	1.9	0.1745	0.1753	W	1.9	0.1755	0.1752
2126	0.1732	0.1743	W	1.9	0.1730	0.1743	W	1.9	0.1730	0.1738	W	1.9	0.1741	0.1730
1325**	0.1705	0.1715	M	3.6	0.1700	0.1715	M	3.6	—					
**$									0.1685		W			
$													0.1681	
**$									0.1668		W			
**$									0.1665		W			
$									—				0.1655	
1327**$	0.1649	0.1660	M	2.8	0.1644	0.1660	M	2.8	—				0.1643	0.1644
2226	0.1608	0.1615	M	1.3	0.1606	0.1615	M	1.3	0.1607	0.1611	M	1.3	0.1609	0.1606
0426	0.1504	0.1513	M	3.3	0.1502	0.1513	M	3.3	0.1502	0.1510	M	3.3	0.1509	0.1506

**denotes the lines which characterize the transtion (β'_0-β''_2)
$ denotes the lines which characterize the transtion (β''_2–β')
V-S: Line of very strong intensity
S: Line of strong intensity
M: Line of medium intensity
W: Line of weak intensity

DOMAINS OF EXISTENCE OF SOLID SOLUTIONS AS A FUNCTION OF THE C_{25} CONCENTRATION AT A TEMPERATURE OF 20°C

We have prepared twenty seven mixtures with increasing C_{25} molar concentrations in order to determine:

i) The solubility domains of C_{25} in the $\beta_0(C_{23})$ and $\beta'_0(C_{23})$ structure of C_{23}.
ii) The domain of existence of the three intermediate phases β''_1, β', β''_2 and the solubility domain of C_{23} in the $\beta_0(C_{25})$ structure at 20°C (Table V).

The terminal solid solution $\beta_0(C_{23})$

The X-ray patterns corresponding to the mixtures with C_{25} concentrations ranging from 0% to 0.5% show the lines of the orthorhombic structure $\beta_0(C_{23})$.

The $\beta'_0(C_{23})$ solid solution

For concentrations of at least 1.5% in C_{25}, the reflections characterizing the $\beta_0(C_{23})$ structure, (1 0 24) and (2 1 23), have completely disappeared (Fig. 1). That is the $\beta'_0(C_{23})$ single-phase domain, whose structure is observed in C_{23} above δ transition.

The β''_1 intermediate solid solution

β''_1 exists as a single-phase for a molar concentration higher than 3% in C_{25}. The $\beta'_0(C_{23})$ reflections have disappeared (Fig. 1). The concentration domain extends up to 5 mole % in C_{25}.

The β' intermediate solid solution

β' exists as a single-phase between 22.25 and 50 mole% of C_{25}. The reflections belonging to β'_1 have disappeared (Fig. 1).

TABLE V

Domains of existence of solid solutions versus *n*-pentacosane concentration at a temperature of 20°C

Molar Concentration (% in n-C_{25})	Solid Solution	Molar Concenration (% in n-C_{25})	Solid Solution
0.5	$\beta_0(n\text{-}C_{23})$	54	$\beta' + \beta''_2$
1	$\beta_0(n\text{-}C_{23}) + \beta'_0(n\text{-}C_{23})$	60	$\beta' + \beta''_2$
1.5	$\beta'_0(n\text{-}C_{23})$	70	$\beta' + \beta''_2$
2	$\beta'_0(n\text{-}C_{23})$	75	β''_2
2.5	$\beta'_0(n\text{-}C_{23}) + \beta''_1$	80	β''_2
3	β''_1	85	β''_2
4	β''_1	88	β''_2
10	$\beta''_1 + \beta'$	90	$\beta''_2 + \beta_0(n\text{-}C_{25})$
20	$\beta''_1 + \beta'$	91.5	$\beta''_2 + \beta_0(n\text{-}C_{25})$
22.25	β'	92	$\beta''_2 + \beta_0(n\text{-}C_{25})$
25	β'	93.5	$\beta''_2 + \beta_0(n\text{-}C_{25})$
30	β'	95	$\beta_0(n\text{-}C_{25})$
40	β'	100	$\beta_0(n\text{-}C_{25})$
50	β'		

The β_2'' intermediate solid solution

β_2'' exists for molar concentrations ranging from 75 to 88 mole % in C_{25}. The reflections belonging to the β' phase have disappeared (Fig. 1). β_2'' and β_1'' show identical X-ray pattern. Then these two phases are isostructural.

The terminal solid solution $\beta_0(C_{25})$

The X-ray patterns made on the mixture with C_{25} concentration ranging from 100% to 95% correspond of the $\beta_0(C_{25})$ orthorhombic structure of C_{25}.

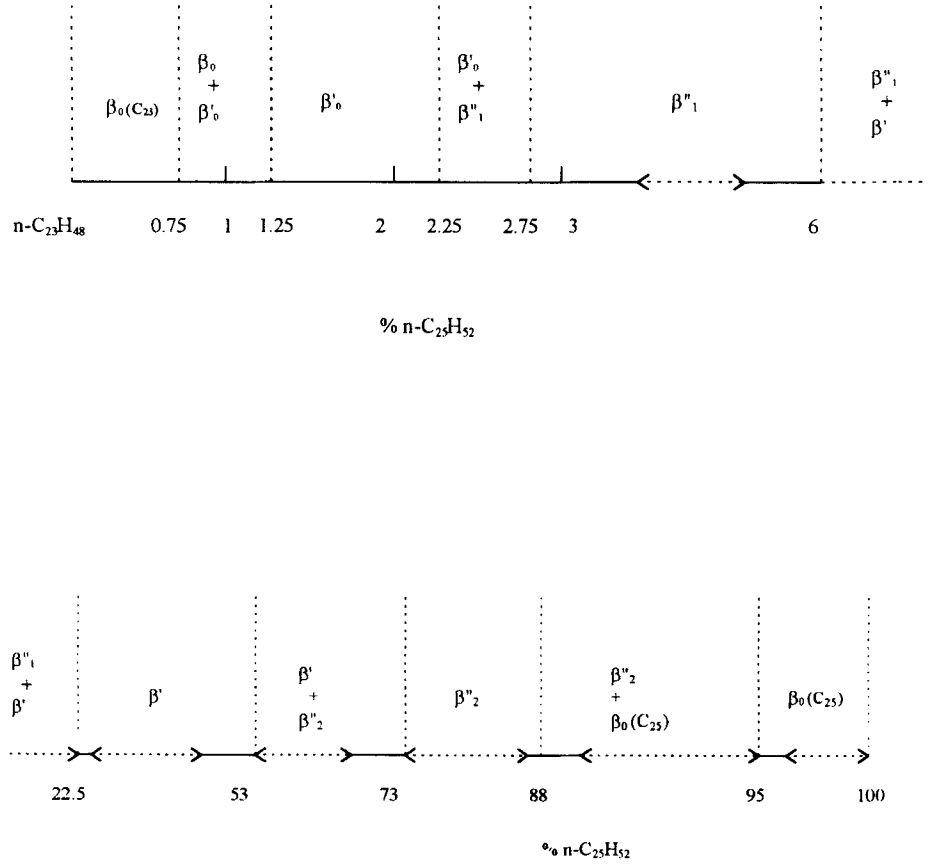

FIGURE 2 Domains of existence of phases for binary mixtures of C_{23}–C_{25} as a function of molar concentration in C_{25} at 20°C.

A COMPARISON BETWEEN β_1'', β_2'' AND β' WITH THE INTERMEDIATE PHASES OBSERVED IN BINARY MIXTURES OF OTHER N-ALKANES

On the basis of powder X-ray diffraction photographs (Fig. 1; Table III and Table IV) the following results are established:

i) the orthorhombic indistinguishable intermediate phases β''_1 and β''_2 are isostructural with the second intermediate solid solution β'', observed in the binary systems $[C_{22}:C_{24}]$[6,7] and $[C_{24}:C_{26}]$[8] and with β''_1, which appears also, in the $[C_{22}:C_{23}]$ and $[C_{23}:C_{24}]$ binary mixtures near the terminal solid solution $\beta'_0(C_{23})$ when the solute concentration increases in C_{23}.[9,32]

ii) the second intermediate phase β' is also isostructural with the first intermediate phases β'_1 and β'_2 observed in the $[C_{22}:C_{24}]$[4,6,7] and $[C_{24}:C_{26}]$ systems[8] and with the first intermediate phase β'_1 detected in the $[C_{22}:C_{23}]$ systems.[32]

CONCLUSION

X-ray diffraction patterns allow us to determine the domains of single-phase existence from 0% to 100% in C_{25}. At 20°C there are (Fig. 1 and Fig. 2):

i) three domains of terminal solid solution.

- $0 < x < 0.75\%$: terminal solid solution $\beta_0(C_{23})$, orthorhombic Pbcm.
- $1.25 < x < 2.25\%$: terminal solid solution $\beta'_0(C_{23})$. It is the orthorhombic structure of C_{23}, observed above the δ transition, (high temperature form of C_{23}).
- $95 \leq x \leq 100\%$ terminal solid solution $\beta_0(C_{25})$, orthorhombic Pbcm.

ii) three domains of intermediate solid solutions:

- $3 \leq x < 6\%$: intermediate solid solution β''_1, orthorhombic.
- $22.25 < x < 53\%$: intermediate solid solution β', orthorhombic.
- $73 < x \leq 88\%$: intermediate solid solution β''_2, orthorhombic. β''_1 and β''_2 are isostructural.

As for binary systems of consecutive even-numbered alkanes, it appears from our work that mixtures of the consecutive odd-numbered $[C_{23}:C_{25}]$ *n*-alkanes do not form a continuous homogeneous solid solution as that was presented in literature.[22] On the contrary, all these *n*-alkanes binary mixtures are molecular alloys and their behaviors present similarities with these of metal alloys.[33]

References

1. P. Barbillon, L. Schuffenecker, J. Dellacherie, D. Balesdent and M. Dirand, *J. Chim. Phys.* **88**, 91 (1991).
2. P. M. Ghoghomu, J. Dellacherie and D. Balesdent, *J. Chem. Thermo.* **21**, 925 (1989).
3. P. M. Ghoghomu, J. Dellacherie and D. Balesdent, *Thermochim. Acta.* **157**, 241 (1990).
4. N. Hasnaoui, J. Dellacherie, L. Schuffenecker, M. Dirand and D. Balesdent, *J. Chim. Phys.* **85**(2), 153 (1988).
5. N. Hasnaoui, J. Dellacherie, L. Schuffenecker, M. Dirand and D. Balesdent, *J. Chim. Phys.* **85**(6), 675 (1988).
6. Z. Achour, J. B. Bourdet, M. Bouroukba and M. Dirand, *J. Chim. Phys.* **89**, 707 (1992).
7. Z. Achour, J. B. Bourdet, M. Bouroukba and M. Dirand, *Thermochim. Acta.* **204**, 187 (1992).
8. Z. Achour, J. B. Bourdet, M. Bouroukba and M. Dirand, *J. Chim. Phys.* **90**, 325 (1993).
9. A. Sabour, J. B. Bourdet, M. Bouroukba and M. Dirand, *Thermochim. Acta.* **249**, 269 (1995).
10. W. R. Turner, *Ind. Eng. Chem. Prod. Res. Develop.* **10**, 3, 238 (1971).
11. R. M. Butler and D. M. McLeod, *The Canadian Journal of Chemical Engineering.* 53 (1961).
12. R. T. Edwards, *Ind. Eng. Chem.* **49**, 740 (1957).
13. G. A. Holder and J. Winkler, *J. Inst. Petrol.* **51**(499), 228 (1965).
14. W. M. Mazee, *J. inst. Petrol.* **35**, 97 (1949).

15. W. M. Mazee, *Analyst Chem. Acta.* **17**, 97 (1957).
16. W. Mazee, *Symp. Adv. Chem. Thermod.* B35–B48 (1958).
17. W. M. Mazee, *Erdol und Kohle.* **13**, 2, 88 (1960).
18. S. P. Srivastava, Jyoti Handoo , K. M. Agrawal and G. C. Joshi, *J. Phys. Chem. Solids.* **54**, 6, 639 (1993).
19. A. E. Smith, *Acta Cryst.* **10**, 802 (1957).
20. H. Luth and S. G. Nyburg, *Mol. Cryst. Liq. Cryst.* **27**, 337 (1974).
21. A. R. Gerson and S. G. Nyburg, *Acta Cryst.* **B50**, 252 (1994).
22. J. J. Retief, D. Wengel and E. G. Boonstra, *J. Appl. Cryst.* **18**, 156 (1985).
23. A. E. Smith, *J. Chem. Phys.* **21**, 2229 (1953).
24. P. W. Teare, *Acta Cryst.* **12**, 294 (1959).
25. R. D. Heyding and K. E. Russel, K. E. Varty, D. St Cyr, *Powder Diffraction* **5**, 2 (1990).
26. A. R. Gerson, K. J. Roberts and J. N. Sherwood, *Acta Cryst.* **B47**, 280 (1991).
27. I. Denicolo, J. Doucet and A. F. Graievich, *J. Chem. Phys.* **78**, 3, 512 (1983).
28. K. Ivon, W. Jeitschko and E. Parthe, *J. Appl. Cryst.* **10**, 73 (1977).
29. G. Ungar and G. Masic, *J. Phys. Chem.* **89**, 1036 (1985).
30. G. Ungar, *J. Phys. Chem.* **87**, 689 (1983).
31. R. G. Snyder and M. Maroncelli, *Science* **214**, 188 (1981).
32. A. Sabour, *PhD Thesis INPL* Nancy (1994).
33. Y. Haget, *J. Chim. Phys.* **90**, 313 (1993).